Metal Binding Sites of H^+-ATPase from Chloroplast and *Bacillus* PS3 Studied by EPR and Pulsed EPR Spectroscopy of Bound Manganese(II)

Clotilde Buy, Guy Girault, and Jean-Luc Zimmermann*

CEA/Saclay, Département de Biologie Cellulaire et Moléculaire, Section de Bioénergétique, Bât. 532, F-91191 Gif-sur-Yvette, France

Received March 4, 1996; Revised Manuscript Received April 8, 1996[⊗]

ABSTRACT: The metal binding sites of isolated F1 ATPase from spinach chloroplasts (CF1) and from the thermophilic bacterium *Bacillus* PS3 (TF1) have been studied by EPR and pulsed EPR spectroscopy using Mn(II) as a paramagnetic probe. After dialysis in the presence of EDTA, purified CF1 retains 0.14 ± 0.07 Mg(II) and approximately 0.75 ± 0.25 ADP. TF1 retains 0.31 ± 0.03 Mg(II) and 0.08 ± 0.01 nucleotide (ADP + ATP) after the same treatment. Supplementing known quantities of Mn(II) to metal-depleted CF1 allowed a spectroscopic characterization of the bound Mn(II) cations, for which the EPR spectra at X- and Q-band are reported. The zero field splitting parameters of Mn(II) are derived from the simulation of the EPR signal recorded at Q-band for a sample supplemented with 0.3 Mn/CF1. The values, $|D| \approx 200 \times 10^{-4}$ cm^{-1} and $|E| \approx 40 \times 10^{-4}$ cm^{-1} suggest that the Mn(II) binds to CF1 in a slightly distorted environment. The ESEEM spectra of complexes of Mn(II) with CF1 were also recorded for different Mn/CF1 ratios. For a complex with 0.8 Mn/CF1, the ESEEM spectrum shows two frequencies at 3.7 and 8.6 MHz that are attributed to the magnetic coupling with ^{31}P with a hyperfine coupling constant of $|A| \approx 5.3$ MHz, reflecting the interaction with a phosphate group from the endogenous ADP molecule. This demonstrates close proximity of the strong affinity metal site M1 and the endogenous ADP binding site N1, and binding of the ADP β-phosphate to the divalent metal cation. For Mn(II) complexes with higher Mn/CF1 ratios, new frequency components below ∼5 MHz are resolved in the spectra in addition to the peaks from ^{31}P. From a comparison of the CF1 spectra and their magnetic field dependence across the Mn(II) EPR line shape with those of Mn(II) complexes with imidazole, glycine, poly-L-lysine, and nucleotide ligands, it is concluded that additional metal binding sites are filled at higher Mn contents and that these involve ^{14}N donors. It is suggested that the most probable set of ligands of the divalent metal(s) for these additional metal sites in CF1 includes a lysine residue, in line with a previous proposal [Houseman, A. L. P., Morgan, L., LoBrutto, R., & Frasch, W. D. (1994) *Biochemistry 33,* 4910−4917]. Similar experiments for a Mn(II) complex with TF1 (0.4 Mn/TF1) showed no interaction with ^{31}P; instead modulations are detected in the ESEEM below ∼5 MHz that are attributed to a ^{14}N ligand. This is tentatively attributed to the deprotonated amine of Lys-162 from a β subunit, on the basis of the structural data available for the mitochondrial F1 complex. Addition of the substrate ATP to this Mn·TF1 complex leads to the formation of a ternary Mn·TF1·ATP complex with coordination of the Mn(II) by a phosphate group from the ATP as judged from the ESEEM results ($|A(^{31}P)| \approx 4.5$ MHz). An increase in the hyperfine coupling constant of ^{31}P of the phosphate bound to Mn(II) to $|A(^{31}P)| \approx 5.1$ MHz is observed after incubation of the ternary complex at room temperature. This is interpreted as a significant rearrangement of the coordination sphere of the Mn(II) in the M1 site of the Mn·TF1·ATP complex and may reflect conformational changes of catalytic significance that occur in the nucleotide binding site during unisite hydrolysis of ATP to ADP by this complex.

F-type H^+-ATPsynthases are widely distributed membrane bound enzymes that catalyze the reversible phosphorylation of adenosine diphosphate (ADP)[1] to adenosine triphosphate (ATP) by using a transmembrane proton gradient as a source of energy. F-type ATPsynthases from *Escherichia coli*, mitochondria, chloroplasts, and *Bacillus* PS3 have been studied most extensively and common structural schemes have been proposed (Futai et al., 1989; Senior, 1990; Cross, 1992). The enzyme complex is composed of two distinct parts. F_0, the membrane-spanning part, mediates proton transport to F_1, the extrinsic part of the enzyme which catalyzes the phosphorylation reaction. The soluble F_1 part that can be isolated from the complex is an ATPase enzyme that only retains the ability to hydrolyze ATP to ADP.

The F_1 part of chloroplast and *Bacillus* PS3 ATPsynthases is composed of five different protein subunits with a stoichiometry $\alpha_3\beta_3\gamma\delta\epsilon$ and bears six nucleotide binding sites (Cross & Nalin, 1982; Wise et al., 1983, Girault et al., 1988). These nucleotide sites can be distinguished by their binding affinities and characteristics and are designated N1−N6 (Bruist & Hammes, 1981; Shapiro et al., 1991). Three of

* Author to whom correspondence should be addressed. FAX: +33 1 6908 8717. E-mail: zimmermann@dsvidf.cea.fr.

[⊗] Abstract published in *Advance ACS Abstracts,* July 1, 1996.

[1] ADP, Adenosine 5′-diphosphate; ATP, adenosine 5′-triphosphate; CF1, F1 ATPase from spinach chloroplast; CW, continuous wave; EDTA, ethylenediaminetetraacetic acid; EPR, electron paramagnetic resonance or, equivalently, electron spin resonance or ESR; ESEEM, electron spin echo envelope modulation; EXAFS, extended X-ray absorption fine structure; FT, Fourier transform; GDP, guanosine 5′-diphosphate; HPLC, high-performance liquid chromatography; MF1, mitochondrial F1; TF1, F1 from *Bacillus* PS3; Tricine, *N*-[hydroxy-1,1-bis(hydroxymethyl)ethyl]glycine; TRIS, 2-amino-2-(hydroxymethyl)propane-1,3-diol.

S0006-2960(96)00532-6 CCC: $12.00

the nucleotide binding sites are catalytic and are believed to be directly involved in the phosphorylation reaction, while three other sites are noncatalytic with much less clear function (Cross, 1988). Nucleotide bound to the catalytic N1 site can only be removed by irreversible denaturation of CF1 (Bruist & Hammes, 1981). Recently, structural data from X-ray crystallography have been reported for the mitochondrial F_1 (MF1) purified from beef heart (Bianchet et al., 1991; Abrahams et al., 1994). The latter structure shows the three α and three β subunits arranged alternatively like the segments of an orange, with the six nucleotide binding sites being asymmetrically positioned (Abrahams et al., 1994). The three catalytic nucleotide binding sites are predominantly positioned in the three β subunits with some contributions from groups in the α subunits. The three noncatalytic sites are made of groups from the α subunits with a minor contribution from groups in the β subunits. Many regions of the crystallographic map in the published data are not very well defined, however, and they do not show enough resolution so as to completely define the protein binding sites for the nucleotides.

Many divalent metal cations, such as Mg(II), Mn(II), Ca(II), and Co(II), have been shown to serve as essential cofactors of the F_1-ATP synthesis and hydrolysis reactions (Hochman & Carmeli, 1981; Frasch & Selman, 1982; Carmeli et al., 1986). In the native enzyme where the natural divalent metal cation is found to be Mg(II), ATP synthesis/hydrolysis is generally believed to be a binding change mechanism, with the metal complexes Mg[ADP] and Mg[ATP] being the substrates, whereas free Mg(II) and free nucleotides are inhibitors of the synthesis/hydrolysis activity [see Boyer (1993) for a review]. However, a recent detailed study on the ATPase activity of CF1 and of the thermophilic *Bacillus* PS3 F_1 complex (TF1) suggests that the hydrolysis rate of the enzyme is best modeled by a function of the concentration of free ATP and that free Mg(II) is an essential activator (Berger et al., 1994; Pezennec et al., 1995). Thus, the role of the metal cation in both the synthesis and hydrolysis mechanism remains obscure.

In the absence of added nucleotides, six binding sites for Mn(II) have been determined on CF1: three of them have cooperative binding properties with an average $K_d \approx 15\ \mu$M, and three are non-interacting with $K_d \approx 47\ \mu$M (Hiller & Carmeli, 1985). From NMR relaxation measurements of water protons, Haddy et al. (1985) identified two high-affinity metal sites with cooperative binding. Further studies by these authors reported a total of three high-affinity sites for divalent metal cations, including a site with endogenous tightly bound Mg(II) (Haddy & Sharp, 1989; Haddy et al., 1989). More recently, structural information on these metal binding sites has been reported from the analysis of the magnetic properties of VO(II) bound to CF1 (Houseman et al., 1994a,b, 1995). These authors reported a first high-affinity binding site, M1, with bound Mg(II) that is difficult to deplete. Two other sites, M2 and M3, could be occupied by exogenous added VO(II) in the presence or absence of nucleotide. The M2 and M3 sites seem to interact with the nucleotide binding sites N2 and N3 (Houseman et al., 1995), and a model for the amino acid side chains involved in metal binding was proposed, based on the amino acid sequence of the mitochondrial enzyme. In addition, the above model predicts that nucleotide binding to a nucleotide binding site involves a change in the ligand set of the VO(II) (Houseman et al., 1995).

In the present study, Mn(II) is used as an EPR paramagnetic probe of the environment and the ligands involved in the Mg(II) binding sites of CF1 and TF1. EPR has already been successfully used to study the metal sites in proteins where the natural metal ion is Mn(II) or is replaced for Mn(II) (Reed & Markham, 1984). In particular, analysis and simulation of the EPR signal at Q-band can provide insights into the coordination symmetry of the Mn(II) site, and in some instances, superhyperfine broadening of the EPR signal with ^{17}O nuclei from coordinated water or other ligands has been detected (Reed & Leyh, 1980; Eads et al., 1988; Latwesen et al., 1992). However, the magnetic coupling with nuclei such as ^{14}N or ^{31}P from metal ligands is usually concealed in the line widths of the EPR signals, precluding further analysis of the coupling parameters of possible ^{14}N or nucleotide phosphate ligands to the Mn(II).

ESEEM spectroscopy is a high-resolution technique based on the pulsed EPR method, that has the potential for detecting the couplings with nuclear spins that remain unresolved in a conventional EPR spectrum (Kevan, 1990). ESEEM has proved to be successful in providing structural insights on the binding pocket of the metal site in a number of Mn(II) containing proteins. These include complexes of Mn(II) with the kinases, creatine (LoBrutto et al., 1986) and pyruvate (Tipton et al., 1989) kinases, tartrate dehydrogenase (Tipton & Peisach, 1991), glutamine synthetase (Eads et al., 1988), a number of lectins (McCracken et al., 1991), and complexes with the human *ras* gene product p21 *ras* (Halkides et al., 1994) and the newly discovered Mn(II) site in cytochrome *c* oxidase (Espe et al., 1995). Coupling with ^{14}N from histidine imidazole bound to Mn(II) gives rise to characteristic ESEEM patterns, and frequencies from nucleotide ^{31}P or nearby ^{2}H in the ^2H_2O enriched material may also be detected. In this context, it is of note that the ESEEM data recorded for the p21 *ras* protein in solution were interpreted in terms of a set of ligands for the Mn(II) site that showed significant differences with that derived in the crystal from the X-ray diffraction data, thus showing that particular insightful and original data may be gained from ESEEM spectroscopy (Halkides et al., 1994). In the present work, the CW EPR spectra at X-band and Q-band of Mn(II) bound to CF1 are reported, together with ESEEM spectra of Mn·CF1 and Mn·TF1 complexes in different stoichiometries, in an attempt to characterize the geometry and the environment of the metal binding sites of these two closely related enzymes. The zero field splitting parameters which are obtained by simulation of the Q-band EPR spectrum indicate that the coordination of Mn(II) bound to the complex has a slightly disturbed octahedral symmetry. The ESEEM spectrum of Mn(II) bound to CF1 with a Mn/CF1 ratio lower than unity shows coupling with a ^{31}P nucleus, probably from the ADP molecule that is tightly bound to the N1 site. This is evidence for metal−nucleotide binding at this site. For higher concentrations of Mn(II), additional sites are filled on CF1, whose ESEEM spectra are indicative of a coupled ^{14}N nucleus that is attributed to a protein ligand. Comparison with ESEEM spectra obtained for complexes of Mn(II) with nitrogen-containing ligands suggests that this protein ligand is more likely the deprotonated terminal amine of a lysine side chain, in line with the earlier report of Houseman et al. (1994a, 1995) using bound VO(II). By contrast, TF1

can be prepared devoid of nucleotide, and the ESEEM spectra of Mn(II) complexes with TF1 only show the interaction with the ^{14}N ligand. Interaction of Mn(II) with ^{31}P is detected in the ESEEM only after addition of exogenous nucleotide to the complex. The significance of these results toward the mechanism of ATP hydrolysis and current structural models of F_1 already published in the literature are discussed.

MATERIALS AND METHODS

Soluble chloroplast ATPase (CF1) was prepared from spinach and extracted by a treatment with EDTA, sucrose, and chloroform and then purified using DEAE cellulose and Protein Pak DEAE 5 PW HPLC columns (Berger et al., 1987). The purified CF1 was stored at 4 °C as a precipitate in ammonium sulfate at 50% saturation. Extraction and purification of TF1 from *Bacillus* PS3 cells were performed as described in Kagawa and Yoshida (1979) with the modifications described by Pezennec et al. (1995). Prior to use, aliquots of the protein precipitate were dialyzed during 24 h against 50 mM TRIS-HCl, 10 mM EDTA, pH 8, followed by another 48 h dialysis against 50 mM TRIS-HCl, pH 8. This treatment was aimed at removing divalent cations bound to the protein complex. The protein was then concentrated to ≥30 mg/mL for the purpose of EPR measurements. Protein concentrations were measured as described (Bradford, 1976) with the Bio-Rad protein assay, using bovine serum albumin as a standard. Mn(II) was added to the metal-depleted protein samples from aqueous solutions of $MnCl_2$, and the samples were immediately frozen in liquid nitrogen, where they were stored until use.

In some experiments, the samples of CF1 were prepared in a different manner: an additional dialysis against 50 mM TRIS-HCl, pH 8, with 1 mM $MnCl_2$ was added after the last dialysis, to potentially fill the metal binding sites on the protein with Mn(II). It was followed by dialysis against the buffer without Mn(II) for various periods of times to remove Mn(II) not bound or loosely bound to the protein.

The Mg(II) content of CF1 and TF1 was determined by atomic absorption spectroscopy using a 2280 Perkin-Elmer apparatus equipped with an HGA 300 graphite furnace.

The concentrations of nucleotides in samples of CF1 and TF1 and the ATPase activity of the isolated proteins were determined using HPLC as described in Berger et al. (1990) and Pezennec et al. (1995) with the following modifications: the stoichiometry of endogenous nucleotides was calculated assuming a molecular weight of 400 000 Da for CF1 (Moroney et al., 1983) and 385 350 Da for TF1 (Ohta et al., 1988). The ATPase activity was measured at 37 °C in a TRIS-SO_4 buffer, pH 8, with 180 μM $MgSO_4$ (or $MnSO_4$, depending on the metal cofactor tested) and 1 mM ATP. Prior to activity measurements, CF1 was activated by incubation in 20 mM Tricine, pH 8, 10 mM dithiothreitol. The incubation was at least 1 h long, at room temperature.

Frozen solutions of Mn(II) complexed with exogenous ligands [^{14}N or ^{15}N imidazole, ^{14}N or ^{15}N glycine, ATP, poly-L-lysine (MW 26 000)] were obtained by dissolving $MnCl_2$ in H_2O:ethanol (75:25) or H_2O:glycerol (55:45) mixtures, and adding the desired ligand with a stoichiometry 500:1 compared to the metal ion for imidazole and glycine, 10:1 for ATP, and 0.14:1 for poly-L-lysine.

EPR spectra at X-band were recorded with a Bruker 200 D spectrometer using a standard TE_{102} cavity. The spectrometer is equipped with a microwave frequency counter (Hewlett Packard 5350B) and an NMR gauss meter (Bruker ER035M). A sample temperature of 10 K was achieved using a liquid helium cryostat (Oxford Instruments). EPR spectra at Q-band were recorded with a Bruker 300 E spectrometer (Prof. G. Calas, Laboratoire de Minéralogie, Université Paris VII) equipped with a cylindrical cavity. The spectra were recorded at ~140 K using a liquid N_2 cryostat. The simulations of the Q-band EPR spectra were performed using a FORTRAN program that was based on the perturbation formulae, including third-order corrections, and on the forbidden transition energies of the Mn(II) paramagnet (Markham et al., 1979; Reed & Markham, 1984). The validity of the program was verified by qualitatively reproducing the characteristic features of EPR spectra at Q-band published in the literature (Reed & Markham, 1984).

For the quantitation of Mn(II) in the EPR samples containing CF1 or TF1, the X-band EPR spectrum of Mn(II) was measured under the same experimental conditions as for the CF1 samples ($T = 10$ K, $P = 2$ mW) for a series of samples prepared with 100 mM TRIS-HCl, pH 8, and a known concentration of Mn(II). The amplitude of the EPR signal was taken as the sum of the intensities of the six major hyperfine lines. The Mn(II) concentration as a function of the amplitude of the EPR signal was obtained from a linear regression of the data points ($R = 0.98$). The concentration of Mn(II) in samples with CF1 and TF1 was determined from this fit, and the Mn/protein ratio was deduced.

Three-pulse (stimulated echo) ESEEM experiments were all carried out at 4.2 K, using a Bruker ER 380 pulsed EPR spectrometer and an Oxford Instruments liquid helium immersion Dewar. In this type of experiment, a sequence of three resonant $\pi/2$ microwave pulses produces a stimulated echo (Kevan, 1990). The echo corresponds to the sample magnetization that is refocused after its decay during the first interpulse time τ. The decay of the magnetization is due to the frequency distribution of the precessions of the individual spin packets that contribute to the resonant EPR line. This distribution originates in particular from unresolved hyperfine and/or quadrupolar couplings of nearby nuclear spins. When the stimulated echo is recorded as a function of the interpulse time T separating the second and third pulses, the amplitude of the echo decays with a time that is characteristic of the longitudinal relaxation time T_1. Modulation functions are sometimes convoluted with this overall decay function of the echo (ESEEM), and they are characterized by frequencies after Fourier transformation, which are nuclear frequencies corresponding to hyperfine and/or quadrupole couplings of nuclei with non-zero spin that are close to the electronic spin. Nuclear state admixture is necessary for the observation of these ESEEM frequencies, and is produced by the anisotropic part of the hyperfine/quadrupole interactions. However, both isotropic and anisotropic hyperfine couplings for a particular nucleus at a particular orientation contribute to the nuclear frequencies that are measured in the ESEEM spectrum. For the experiments reported in this work, the interpretation is further complicated by the high-spin multiplicity of the Mn(II) ion ($S = 5/2$), and the possibility of couplings with nuclei with $I \geq 1$ (e.g., ^{14}N). The ESEEM frequencies reported here are thus interpreted as hyperfine coupling constants $|A|$ for which the isotropic and anisotropic parts are not determined.

Table 1: Metal Ions and Nucleotides Bound to CF1 and TF1

sample and treatment	mole ratio of metal/CF1		mole ratio of (ADP+ATP)/CF1[a]
	Mg[b]	Mn[c]	
CF1/EDTA+Mn(II)#1[d]	0.14 ± 0.07	0.8	0.75 ± 0.25
CF1/EDTA+Mn(II)#2[d]		4.0	
CF1/EDTA/Mn(II)/d6[e]		5.6	
CF1/EDTA/Mn(II)/d24[f]		0.3	
TF1/EDTA+Mn(II)#1[g]	0.31 ± 0.03	0.4	0.08 ± 0.01
TF1/EDTA+Mn(II)#2[g]		3.0	

[a] Determined by HPLC. Average of 18 measurements on all of the CF1 samples and six on the TF1 samples. [b] Determined by atomic absorption spectroscopy. Average of eight measurements on the four CF1 samples and five measurements on the two TF1 samples. [c] Determined by quantitation of the EPR signal. [d] CF1 was dialyzed during 24 h against buffer with 10 mM EDTA, then against buffer without EDTA, and subsequently supplemented with different amounts of $MnCl_2$ (see Materials and Methods). [e] CF1 was dialyzed against buffer with 10 mM EDTA, then against buffer with 1 mM $MnCl_2$, and then against buffer for 6 h (see Materials and Methods). [f] CF1 was dialyzed against buffer with 10 mM EDTA, then against buffer with 1 mM $MnCl_2$, and then against buffer for 24 h (see Materials and Methods). [g] TF1 was dialyzed during 24 h against buffer with 10 mM EDTA, then against buffer without EDTA, and subsequently supplemented with different amounts of $MnCl_2$ (see Materials and Methods).

A phase cycling algorithm was used to eliminate the contributions from secondary echoes to the three-pulse echo envelope (Fauth et al., 1986). The τ values were chosen as twice the inverse of the proton Larmor frequency for the external magnetic field strength so that modulations due to weakly coupled protons were suppressed in the stimulated echo signal (Mims & Peisach, 1981). Fourier transformation of the ESEEM data sets (typically 800 data points with increment $\Delta T = 8$ ns) was performed after reconstruction of the $n = (\tau + T_{start})/\Delta T$ missing data points using a program based on a modified version of the deadtime reconstruction algorithm published by Mims (1984).

RESULTS

Characterization of the Metal Binding Site M1 in CF1 and TF1. CF1 isolated from spinach contains bound Mg(II) cations and nucleotides. When dialyzed in the presence of EDTA (see Materials and Methods), the CF1 complex contains very little remaining divalent metal cations as judged by atomic absorption spectroscopy. Table 1 shows that after the two 24 and 48 h dialysis periods in the presence of 10 mM EDTA, CF1 contains approximately 0.14 ± 0.07 Mg(II) and 0.75 ± 0.25 nucleotide per CF1. The treatment performed here seems to have depleted Mg(II) from all of the metal binding sites that exist on CF1, in particular the three binding sites with relatively strong affinity and known as M1−M3 that have been described in previous studies (Hiller & Carmeli, 1984; Houseman et al., 1994a). Approximately one ADP molecule remains bound to CF1, and this is likely to correspond to the tightly bound catalytic N1 site (Bruist & Hammes, 1981; Shapiro et al., 1991).

The ATPase activity of metal-depleted CF1 that can be measured after activation with dithiothreitol in the presence of Mg(II) or Mn(II) ions [~1.0 and ~2.1 μmol of ADP min^{-1} (mg of protein)$^{-1}$ respectively] indicates that Mn(II) cations can substitute extremely efficiently for Mg(II) in the hydrolysis reaction [see Hochman et al. (1976)]. For the EPR spectroscopic studies described below, Mn(II) was added to a sample that had experienced the metal depletion treatment

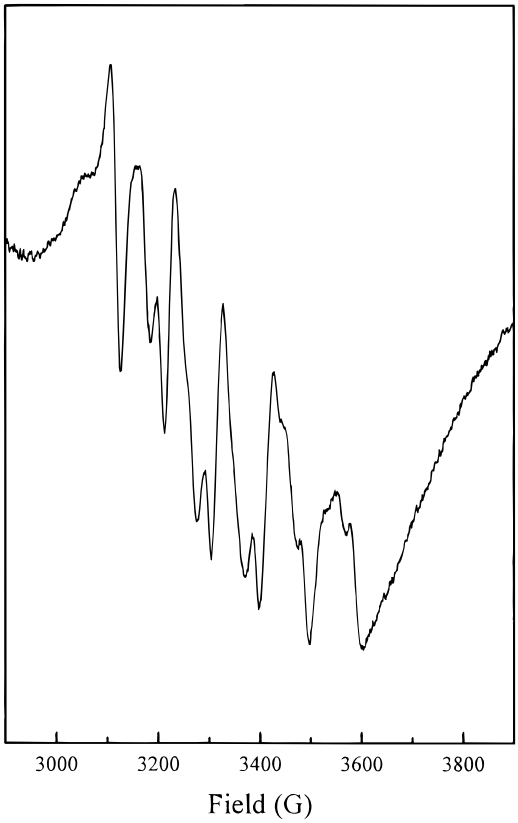

FIGURE 1: X-band EPR spectrum of a sample containing metal-depleted CF1 and supplemented with exogenous Mn(II) (Mn/CF1 ratio: 0.3, see text). Experimental conditions were the following: temperature, 10 K; microwave power, 2 mW; microwave frequency, 9.423 GHz; modulation amplitude, 9.65 G.

mentioned above. For this purpose, CF1 was incubated in the presence of Mn(II) and then dialyzed in the same buffer without any divalent metal cation. For the last step, the buffer was changed several times so that the remaining concentration of Mn(II) in the buffer after equilibrium (calculated concentration < 0.5 μM) was negligible compared with that in the sample (~50−300 μM, deduced from the EPR data). Thus the EPR signals that could be detected in the samples prepared in this manner could be assigned to Mn(II) bound to CF1. Figure 1 shows the X-band EPR spectrum of a sample of CF1 that was dialyzed for 24 h (0.3 Mn/CF1; see Table 1). The typical EPR signal of Mn(II) with six major hyperfine lines centered around $g \approx 2$ originates from the hyperfine splitting of the central transition $M_S = -1/2$ to $M_S = -1/2$ of the $S = 5/2$ paramagnet with $I = 5/2$ of the ^{55}Mn nucleus. A contribution from the other four fine structure transitions ($M_S = -5/2$ to $-3/2$, $M_S = -3/2$ to $-1/2$, $M_S = +1/2$ to $+3/2$, and $M_S = +3/2$ to $+5/2$) can also be detected in the spectrum, especially the structureless features below ~3100 G and above ~3600 G. In fact, the spectrum at X-band is dominated by forbidden transitions of the type $|-1/2,m> \leftrightarrow |+1/2,m\pm1>$ that gain transition probability owing to the zero field splitting interaction. The EPR spectrum of Mn(II) is usually simplified when measured at a higher microwave frequency like Q-band (~35 GHz) because the relative magnitude of the forbidden transitions is smaller. In addition, the electron Zeeman energy is approximately four times larger at Q-band than at X-band, whereas the energy of the hyperfine interactions is unchanged, and consequently the effects of possible hyperfine anisotropy in the spectrum are relatively smaller. In fact,

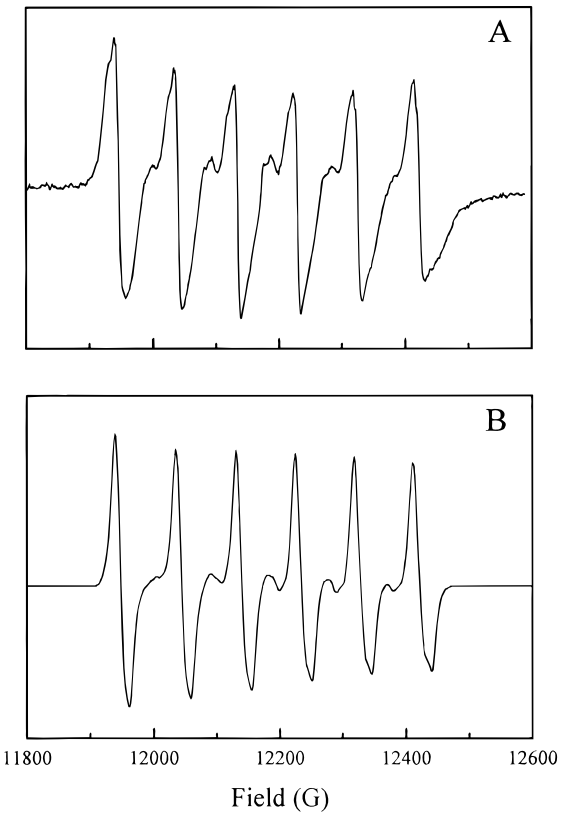

FIGURE 2: (A) Q-band EPR spectrum of the same sample as that studied in Figure 1. Experimental conditions: temperature, 140 K; microwave power, 1 mW; microwave frequency, 34.12 GHz; modulation amplitude, 5 G. (B) Simulation of the experimental spectrum in A using the following EPR parameters: $g_{iso} = 2.0$, $|D| = 200 \times 10^{-4}$ cm^{-1}; $|E| = 40 \times 10^{-4}$ cm^{-1}; $A_{iso}(Mn) = 88 \times 2.10^{-4}$ cm^{-1}, and a line width of 7 G.

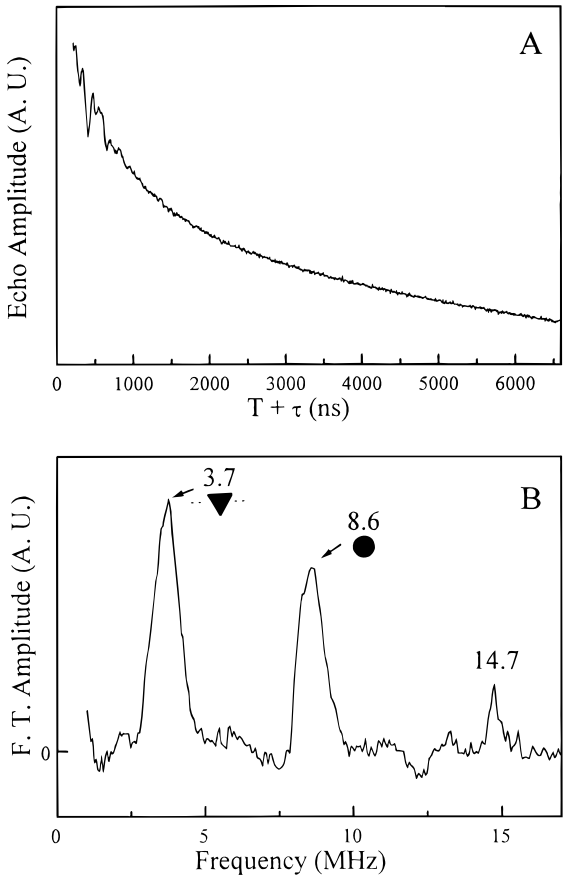

FIGURE 3: Three-pulse ESEEM signal (A) and cosine Fourier transform (B) of Mn(II) bound to CF1 (0.8 Mn/CF1). The data were obtained at a temperature of 4.2 K, a microwave frequency of 9.65 GHz, and a magnetic field setting of 3460 G. The interpulse time τ was 136 ns, and the time interval between successive spin echo pulse sets was 1.53 ms.

the Q-band EPR spectrum of a Mn(II) site may be simulated with relatively good confidence by using a perturbation approach for the zero field splitting terms in the Hamiltonian and the contribution of the forbidden transitions to the EPR line shape (Reed & Markham, 1984). The Q-band EPR spectrum of a CF1 sample with 0.3 Mn/CF1 together with the simulation that was judged best are shown in Figure 2. The simulated spectrum was obtained with a Mn isotropic hyperfine coupling constant, $|A_{iso}| \approx 88.2 \times 10^{-4}$ cm^{-1}, and the following zero field splitting parameters, $|D| \approx 200 \times 10^{-4}$ cm^{-1} and $|D| \approx 40 \times 10^{-4}$ cm^{-1}. These latter parameters are relatively small when compared with those found for Mn(II) sites in proteins [$|D| \approx (100-1300) \times 10^{-4}$ cm^{-1}; see Reed and Markham (1984)], and they indicate a relatively high degree of symmetry for the Mn(II) site in CF1. The shape of the spectrum at Q-band and the results of the simulation indicate, however, a small but significant deviation from octahedral symmetry for Mn(II) and demonstrate that the added Mn(II) cation binds to CF1 in a specific environment with a symmetry lower than octahedral.

EPR spectra at both X- and Q-bands were also collected for CF1 samples depleted of Mg(II) and nucleotides by the EDTA treatment and supplemented with Mn(II) in known amounts. The EPR spectra of these samples were very similar with those shown in Figures 1 and 2, indicating that Mn(II) binds to metal-depleted CF1 in specific environments that can probably be identified as the native Mg(II) binding sites in the absence of nucleotides. Although this approach could not be used to discriminate by EPR, metal binding sites with different affinities that would sequentially be filled by added Mn(II) (see below however), the results reported here for samples with Mn concentrations ranging from 0.3 to 3 Mn/CF1 strongly suggest that the metal sites observed by EPR correspond to the high-affinity binding sites known as M1 to M3 (Houseman et al., 1994a).

Insights into the binding pocket(s) of Mn(II) in CF1 may be gained by studying the coupling of magnetic nuclei in the vicinity of Mn(II), especially those involved as ligands to the metal cation. As mentioned above, this information, which is usually lost in the large inhomogeneously broadened line shapes of the CW EPR spectra, can be recovered from the data of ESEEM spectroscopy, which is a high-resolution technique (Kevan, 1990). Magnetic nuclei that are in the close environment of the Mn(II) ($<$6 Å) may give rise to a peak at their Larmor frequency after Fourier transformation of the data or to a typical frequency pattern when the hyperfine coupling $|A|$ with the Mn(II) paramagnet is sufficiently large. As mentioned above, metal cation binding to CF1 may involve ^{14}N from protein ligands, ^{31}P from the bound or added nucleotides, and ^{1}H from bound or nearby H_2O.

A typical three-pulse ESEEM spectrum measured at 3460 G for a CF1 sample with added Mn(II) (0.8 Mn/CF1) reveals two main peaks at ~3.7 and ~8.6 MHz together with a smaller peak at 14.7 MHz (Figure 3). The latter peak arises from weakly coupled protons in the vicinity of the bound Mn(II) ion, and its intensity is largely diminished in Figure

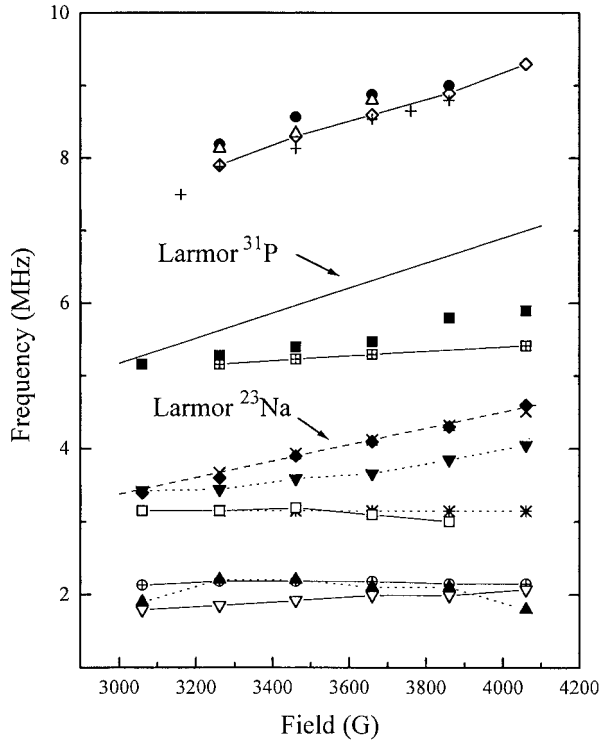

FIGURE 4: Magnetic field dependence of the ESEEM frequencies for complexes of Mn(II): CF1 (0.8 Mn/CF1; Figure 3B), ▼ and ●; TF1 with ATP (0.4 Mn/TF1 and 1 ATP/TF1, Figure 5B and C, respectively), + and △; CF1 (4 Mn/CF1; Figure 6B), ▲; glycine (Figure 7A), * and ×, ⊕, and crossed squares; imidazole (Figure 7B), ▽, □, and ■; ATP (Figure 7C), ◇ and ◆. Frequency values are obtained from spectra recorded under conditions similar to Figures 3, 5, and 7. The straight lines represent the calculated Larmor frequencies for ^{23}Na (dashed line) and ^{31}P (solid line).

3 because of the choice of τ. Control samples with Mn(II) but without CF1 showed ESEEM spectra with only the frequency from weakly coupled protons (not shown). This indicates that the spectrum in Figure 3B arises from Mn(II) bound in a specific environment and confirms that in the CF1 sample, Mn(II) is bound to CF1. To understand the origin of the two main peaks at ∼3.7 and ∼8.6 MHz, ESEEM spectra were recorded for different magnetic field settings throughout the broad EPR absorption line shape of Mn(II) (typically 3100−4100 G), and the frequency positions of the ESEEM peaks were studied. Figure 4 shows that the magnetic field dependence of the 8.6 MHz peak (solid circles) is roughly parallel to that of the Larmor frequency of ^{31}P. Hyperfine coupling of the ^{31}P nucleus ($I = {}^1/_2$) with an electronic spin with $S = {}^1/_2$ may give rise to two peaks in the ESEEM, at frequency values given by $|\nu_L \pm A/2|$, where ν_L is the ^{31}P Larmor frequency (∼5.97 MHz at 3460 G) and A is the hyperfine coupling. Although the coupling with the $S = {}^5/_2$ spin may give rise to additional frequency components in the ESEEM (Larsen et al., 1993; LoBrutto et al., 1993), the observed field dependence of the 8.6 MHz peak for the CF1 sample suggests that this feature arises from coupling with ^{31}P with $A \approx 5.3$ MHz for the $M_S = -{}^1/_2$ manifold of the $M_S = \pm{}^1/_2$ electronic transition[2] (Larsen et al., 1993). The ESEEM peaks at ∼8 MHz that are observed for magnetic field values above 3600 G probably arise from couplings with electronic transitions of the type $M_S = \pm{}^1/_2$ to $M_S = \pm{}^3/_2$ [see Larsen et al. (1993)]. In this region, the magnetic field dependence of the ESEEM frequencies ν_i might be more complicated than the linear dependence expected for the $M_S = \pm{}^1/_2$ transition, and a more sophisticated interpretation might be obtained by plotting the ν_i as $\nu_i^2 - \nu_L^2$ vs $\zeta_i \nu_L$, where the sign variable ζ_i refers to the sign of M_S in the manifold associated with ν_i. In fact, Larsen et al. (1993) have shown that in such a plot, the ESEEM data from ^{31}P of the nucleotide β-phosphate measured for a Mn(II) complex of p21 *ras* with GDP displayed a small yet significant deviation from the linear dependence, with a curvature that could be predicted theoretically for the $M_S = \pm{}^1/_2$ to $M_S = \pm{}^3/_2$ transitions. The ESEEM data shown in Figure 4 for the Mn(II) complex with CF1 do not allow such a detailed interpretation however, yet the general trend shown by the data above 3600 G, especially the continuous and monotonous magnetic field dependence is also consistent with the assignment of the ESEEM peaks at ∼8 MHz to the coupling with ^{31}P. The hyperfine coupling with a magnitude $|A| \approx 5.3$ MHz with ^{31}P mentioned above may arise if Mn(II) is coordinated by a phosphate group. Additional evidence for this interpretation is given below, and it is concluded that the strong-affinity metal binding site M1 involves phosphate binding by a nucleotide. Because no exogenous nucleotide was added to the CF1 sample, it is likely that the nucleotide bound to Mn(II) is the residual ADP molecule that is tightly bound to CF1 (N1 site).

The origin of the 3.7 MHz peak in Figure 3 is less clear and cannot be readily determined from the magnetic field dependence shown in Figure 4 (▼). One possibility is that it may correspond to the ^{31}P companion peak (corresponding to the $M_S = +{}^1/_2$ manifold for $A = +5.3$ MHz) of the line at 8.6 MHz which may be expected in this frequency region. However, the slope of the linear fit (Figure 4) is smaller than that predicted for ^{31}P coupled with $M_S = +{}^1/_2$. Because sodium cations are present in the buffer, it was thought that coupling of Mn(II) with a nearby ^{23}Na nucleus might give rise to this peak at 3.7 MHz. However the magnetic field dependence of the peak does not favor this assignment (^{23}Na Larmor frequency: $\nu_L \approx 3.9$ MHz at 3460 G). In fact, it has been shown that a range of transitions in the frequency region 2−5 MHz can be observed for Mn(II) complexes with nucleotides, with no obvious assignment in terms of nuclear transitions of ^{31}P (Larsen et al., 1993; Halkides et al., 1994). Thus, a provisional assignment for the 3.7 MHz peak in Figure 3 is that it arises from bound nucleotide, although other contributions from ^{23}Na or ^{14}N cannot be completely ruled out.

When CF1 is depleted of its ϵ subunit (CF1-ϵ), it does not require additional activation for ATP hydrolysis to proceed, contrary to CF1 with ϵ (Richter et al., 1984). Because this activation of the CF1 enzyme complex might correspond to modifications in the nucleotide and/or metal cation binding pocket on CF1, the ESEEM spectrum was recorded for a complex of CF1-ϵ with 1 Mn/CF1. The spectrum was virtually identical with that shown in Figure 3 for the intact CF1 complex, with the 3.7 and 8.6 MHz peaks attributed to coupling with the bound ADP, and with no indication of changes in the ligation of the Mn(II) in the M1 site following depletion of the ϵ subunit (not shown).

The F1 complex prepared from *Bacillus* PS3 (TF1) under conditions that are similar with those used for CF1 (i.e., dialysis against a buffer containing EDTA) contains very little remaining metal cations [0.31 ± 0.03 Mg(II) per TF1,

[2] Or the $M_S = +{}^1/_2$ manifold if A is negative.

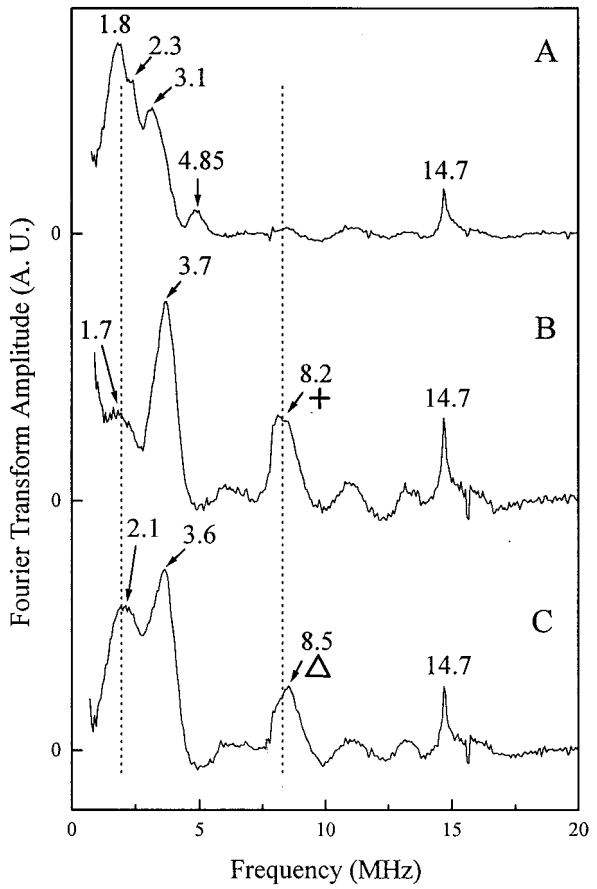

FIGURE 5: Three-pulse FT ESEEM spectra of Mn(II) bound to TF1 (0.4 Mn/TF1) (A), with added ATP (1 ATP/TF1) (B), and subsequently incubated for 15 min at room temperature (C). Spectrometer settings were the same as for Figure 3 except a microwave frequency of 9.58 GHz.

Table 1]. In addition, virtually no nucleotide is retained by TF1 [0.08 ± 0.01 (ADP+ATP) per TF1, Table 1], a property that has been described earlier (Ohta et al., 1980). This situation contrasts with that in CF1, for which one ADP molecule is found to be tightly bound, even after dialysis against EDTA (see above). Because it is shown above that the tightly bound ADP molecule in the N1 site binds to the Mn(II) ion in the M1 site, it seemed interesting to study the binding of Mn(II) to TF1 in a stoichiometric complex of TF1 and Mn(II) and the protein environment in such a complex. Figure 5A shows the three-pulse ESEEM spectrum of a sample of TF1 with added Mn(II) (0.4 Mn/TF1). This spectrum is dominated by a large peak with maximum at 1.8 MHz, a shoulder at 2.3 MHz, and a second component at 3.1 MHz. A smaller peak at 4.85 MHz is also present in the spectrum. It can be immediately noted that the large peaks detected in Figure 3B for the analogous CF1 complex with the 0.8 Mn/CF1 stoichiometry and attributed to the interaction with ^{31}P are absent in the spectrum of TF1. This is not surprising in view of the nucleotide content of TF1. The frequency pattern in Figure 5A resembles that displayed by complexes of Mn(II) with nitrogen-containing ligands (see below), and a provisional interpretation for the ESEEM of TF1 with the 0.4 Mn/TF1 stoichiometry is that the Mn(II) cation is chelated by nitrogen-containing ligands from the TF1 complex.

An additional difference in the enzymatic properties of TF1 compared with those of CF1 is that TF1 does not require activation to drive the hydrolysis of ATP. Thus it might be envisioned to directly follow the steps leading to ATP hydrolysis by studying the environment of Mn(II) by ESEEM spectroscopy after addition of the substrate to the binary complex Mn·TF1 studied above. When this experiment was performed, in an attempt to potentially form a ternary complex, Mn·TF1·ATP, a different frequency pattern was observed in the ESEEM, showing that, indeed, such a ternary complex does form. Figure 5B shows the ESEEM spectrum of the Mn·TF1 sample (0.4 Mn/TF1) with an ATP/TF1 ratio of 1. ATP was added to the Mn·TF1 sample at 4 °C, and the sample was rapidly frozen to liquid nitrogen temperature. Very interestingly, the spectrum shows two large new peaks at 3.7 and 8.2 MHz, that were absent before addition of ATP. The magnetic field dependence of the 8.2 MHz peak suggests that it originates from the interaction with a ^{31}P nucleus (+ in Figure 4), with $|A| \approx 4.5$ MHz (Table 2), showing that phosphate derived from the added ATP molecule binds to the Mn(II), probably after exchange of a native protein ligand or a H_2O molecule. As mentioned above, the spectrum in Figure 5B was obtained for a sample of a Mn·TF1·ATP complex that was rapidly frozen after addition of ATP. However, when the sample with the ternary complex was left to incubate for 15 min at room temperature before freezing to liquid nitrogen temperature and the ESEEM spectrum recorded thereafter, a somewhat different frequency pattern was observed (Figure 5C). In this new spectrum, the two ^{31}P features of the spectrum in Figure 5B are still present, but the high-frequency peak at 8.2 MHz has shifted to a higher frequency at ~8.5 Mhz. This shift suggests that the hyperfine coupling between the Mn(II) and the ^{31}P has increased from $|A| \approx 4.5$ to ~5.1 MHz (Table 2), perhaps reflecting a change or a rearrangement of the nucleotide ligand to the Mn(II). Additional points for the interpretation of the shift of the ^{31}P peak will be given below.

Table 2: ESEEM Frequencies and Hyperfine Couplings with ^{31}P Observed in Mn(II) Sample

sample	^{31}P frequencies (MHz)	$\|A(^{31}P)\|$ (MHz)	attribution
CF1/EDTA+Mn(II)#1	3.7 (?); 8.6	5.3	ADP
Mn·ATP	3.9 (?); 8.3	4.7	ATP
TF1/EDTA+Mn(II)+ATP#1	8.2	4.5	ATP
TF1/EDTA+Mn(II)+ATP#1+ incubation	8.5	5.1	ATP or ADP

It is not completely clear from the spectra in Figure 5B and C whether the peaks at 1.8 and 3.1 MHz that are attributed to ^{14}N ligands of Mn(II) in the absence of ATP (Figure 5A) are still present after addition of the nucleotide. It is possible that the features culminating at 1.7 and 2.1 MHz in Figure 5B and C, respectively, correspond to these ^{14}N frequencies. However, because the frequency patterns are so much dominated by the large ^{31}P peaks from the added ATP, it cannot be concluded whether the Mn(II) ligand with ^{14}N couplings is still a ligand after ATP addition or if it is this ligand that is replaced by a phosphate group from ATP.

Characterization of Additional Metal Binding Sites (M2 and M3) on CF1 and TF1. For CF1 samples treated with EDTA and supplemented with higher concentrations of Mn(II), quite different ESEEM spectra could be recorded. Figure 6 (panels A and B) shows the three-pulse ESEEM and corresponding spectrum measured at 3460 G for a CF1 sample containing 4 Mn/CF1. Comparison with the spec-

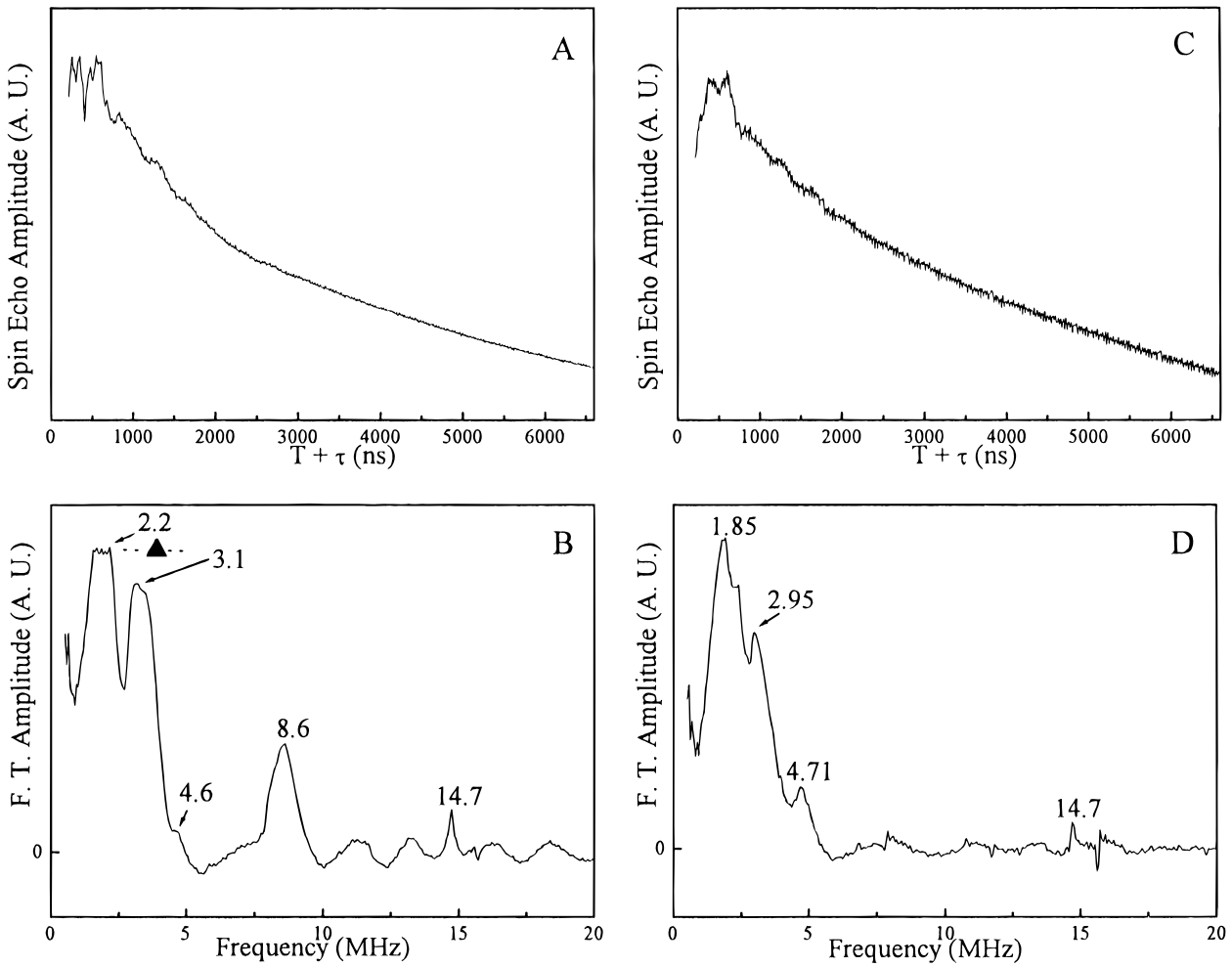

FIGURE 6: Three-pulse ESEEM signals (A and C) and cosine Fourier transforms (B and D) of Mn(II) bound to CF1 (4 Mn/CF1, A and B) and Mn(II) bound to TF1 (3 Mn/TF1, C and D). Spectrometer settings were the same as for Figure 3, except a microwave frequency of 9.68 GHz was used for C and D.

trum of CF1 with 0.8 Mn/CF1 in Figure 3 shows that the ^{31}P peak at 8.6 MHz is still present but that additional peaks at ~2.2 and ~3.1 MHz are resolved. The relative intensity of the 8.6 MHz peak compared with the two large components at 2.2 and 3.1 MHz was somewhat variable from sample to sample (see below). An additional shoulder at ~4.6 MHz is also visible at the high-frequency edge of the 3.1 MHz peak. It is also highly probable that the 3.7 MHz peak in Figure 3 is also present here, although it is probably masked by the more intense 3.1 MHz peak. A TF1 sample prepared in the same manner (3 Mn/TF1) was also examined, and its ESEEM spectrum is shown in Figure 6 (panels C and D). It is readily seen that the 8.6 MHz peak arising from the ^{31}P of bound ADP is absent from the spectrum and also probably the other ^{31}P peak at 3.7 MHz. As mentioned above, quantitation of the nucleotides bound to TF1 shows that contrary to CF1, the TF1 complex can be isolated with virtually no bound ADP (Table 1). This result confirms the assignment of the 8.6 MHz peak to coupling with ^{31}P from phosphate of the bound ADP and probably that of the 3.7 MHz peak also. Besides the ^{31}P peaks, the rest of the spectrum of TF1 is very similar to that of CF1, with two major peaks at ~2 and ~3 MHz and a smaller component at ~4.7 MHz (Figure 6 D), and they probably have the same origin. The pattern of frequency peaks at ~2, ~3, and 4.7 MHz bears some resemblance with spectra reported in the literature for Mn(II) sites with ^{14}N donors (Espe et al., 1995, and references therein), suggesting that the two additional metal binding sites revealed in these samples [M2 and M3 sites, see Houseman et al. (1994a)] may involve ^{14}N ligands. In fact, the ESEEM spectrum of VO(II) bound to CF1 has been interpreted in terms of a ^{14}N ligand (Houseman et al., 1994a). In order to test and substantiate this hypothesis for Mn(II) bound to CF1, and to potentially assign the frequency patterns in Figure 6B and D to a specific ligand set, the ESEEM spectra of Mn(II) in frozen solution and complexed with different nitrogen-containing ligands were studied. Although the origin of the ESEEM frequency pattern arising from ^{14}N coupled to Mn(II) is currently not yet understood, in particular owing to the high spin multiplicity of the Mn(II) ion with $S = {}^5/_2$, some insights may be gained from the qualitative comparison of the spectra with those of Mn(II) with known ligands.

Figure 7 shows the spectra of frozen solutions of Mn(II) complexed with glycine (panel A), imidazole (panel B), and ATP (panel C), respectively. Mn(II) complexed with glycine at pH = 10 displays a frequency pattern with peak maxima at ~2.15, 3.15, 3.9, and 5.2 MHz. Apart from the peak at 3.9 MHz that can be attributed to weakly coupled ^{23}Na nuclei (see below), this frequency pattern is likely to originate from coupling with the primary amine ^{14}N of glycine coordinating the Mn(II) ion, as ^{14}N is the only atom (besides ^{1}H) of the ligand with a non-zero nuclear spin. In fact, when the sample was prepared at pH = 4.75, where the amine is more likely

to be protonated and therefore less likely to coordinate the Mn(II), no modulation besides that corresponding to the ^{1}H Larmor frequency was observed in the ESEEM (not shown). In addition, a very different frequency pattern was observed for Mn(II) complexed with ^{15}N glycine at pH = 10 (not shown), confirming the assignment of the frequency peaks of Figure 7A to coupling of the coordinated amine ^{14}N with Mn(II). An EPR sample prepared at pH 9.1 with poly-L-lysine as ligand gave rise to an ESEEM spectrum very similar with that shown in Figure 7A (not shown). In this latter case, modulations are also likely to arise from the ^{14}N of the deprotonated side chain amines of the lysines that coordinate the Mn(II) ion. The sample with ^{14}N imidazole gives also rise to two low-frequency peaks, at 1.9 and 3.15 MHz, but also to a high-intensity and well-resolved sharp peak at 5.4 MHz (Figure 7B), similar to what has been reported for Mn(II) with imidazole type ligands (McCracken et al., 1991). Accordingly, the ESEEM spectrum of Figure 7B is assigned to coupling with the ^{14}N donor of the imidazole ligand. It is of note that the relatively intense peak at 5.4 MHz in Figure 7B is absent from both the spectra with either TF1 (Figures 5A and 6D), CF1 (Figure 6B), or glycine (Figure 7A), suggesting that the environment of a ^{14}N ligand to Mn(II) in CF1 may be closer to that of ^{14}N in glycine or lysine. The spectrum of Mn(II) complexed with ATP is rather different from the others and is dominated by two peaks at ~3.9 and 8.3 MHz (Figure 7C).

In an attempt to assign more precisely the origin of the different ^{14}N peaks shown in Figure 7, the magnetic field dependence of these features has been studied. Figure 4 displays plots of the FT frequencies in the ESEEM spectra as functions of the magnetic field. The field dependence of the 8.3 MHz peak in the spectrum of Mn(II) with ATP shows that ^{31}P atoms from ATP are coupled with $|A| \approx 4.7$ MHz (see above). Although it is possible that some transitions of ^{31}P may contribute to the peak at 3.9 MHz in the ATP sample, it is readily seen from the graph in Figure 4 that the 3.9 MHz peak occurs at the Larmor frequency of ^{23}Na and with its expected dependence on the magnetic field. Because the sample of Mn(II) with ATP was prepared with the sodium salt of ATP, the peak at 3.9 MHz in the ATP spectrum is assigned to dipolar coupling of Mn(II) with ^{23}Na (the peak at 3.9 MHz in the glycine sample is attributed to coupling with ^{23}Na for similar reasons).

The field dependence of the two prominent peaks at 2.2 and 3.1 MHz in the CF1 sample with 4 Mn/CF1 is also displayed in Figure 4. In fact these peaks, and the corresponding peaks in the TF1 sample, appear to be virtually field independent, just like the corresponding peaks in the glycine and imidazole samples. This reinforces the assignment of these peaks to couplings of Mn(II) with ^{14}N in a manner that is similar with both the Mn(II) imidazole and the Mn(II) glycine complexes. This is taken as evidence that some of the CF1 and TF1 metal binding sites involve a ^{14}N ligand. The imidazole and glycine spectra both show two peaks at ~2 and ~3 MHz that are field independent. The sample with the imidazole ligand shows an additional sharp ^{14}N peak at 5.4 MHz, whose frequency shows a slight variation with the magnetic field, but which is much less intense in the glycine sample. Because the ESEEM spectra of CF1 and TF1 are more similar with the latter, it is suggested that the ^{14}N ligand in the metal site(s) of CF1 and TF1 originates from a primary amine, perhaps the terminal deprotonated amine of a lysine side chain rather than from a histidine imidazole.

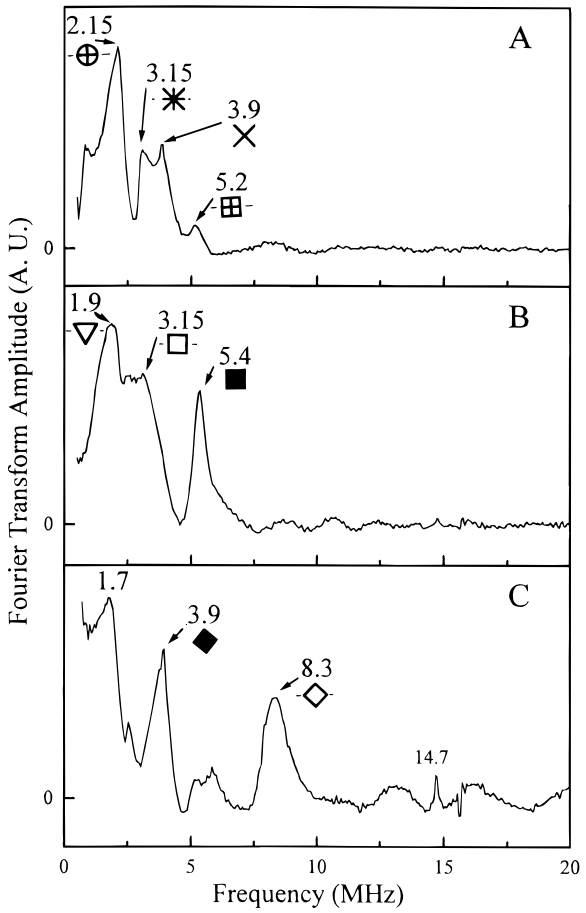

FIGURE 7: Three-pulse FT ESEEM spectra for frozen solution samples of Mn(II) complexed with glycine (A), imidazole (B), and ATP (C). Spectrometer settings were the same as for Figure 3, except a microwave frequency of 9.68 GHz.

The assignment of the 8.6 MHz peak to coupling of Mn(II) with the phosphate from ADP in the N1 site (which is probably the coordinated β-phosphate of ADP) is substantiated by the following observation: ESEEM spectra were recorded for CF1 samples containing increasing Mn/CF1 ratios. The three-pulse ESEEM of samples with ≥1 Mn/CF1 were qualitatively the same as that shown in Figure 7 for 4 Mn/CF1 (not shown). However, the height of the peak at ~2 MHz relative to that of the 8.6 MHz peak increased with increasing Mn/CF1 ratios (Figure 8), just as would be expected if successive metal sites were filled on CF1, starting with the first site with a nucleotide ligand and characterized by the 8.6 MHz feature, and then at least two additional binding sites with lysines as ^{14}N donors (the ~2 MHz feature). These two metal binding sites probably correspond to the M2 and M3 sites described by Houseman et al. (1994a).

Three-pulse ESEEM experiments aimed at determining the changes in the M2 and M3 metal binding sites that may accompany the removal of the ϵ subunit from CF1 were also performed. The three-pulse ESEEM spectra of a sample of CF1-ϵ with added Mn(II) (3 Mn/CF1-ϵ) were virtually identical with those shown in Figure 6B for intact CF1 (not shown), suggesting that the possible changes in the Mn(II) coordination may not be detectable by ESEEM or that no change at all occurs at the metal binding sites.

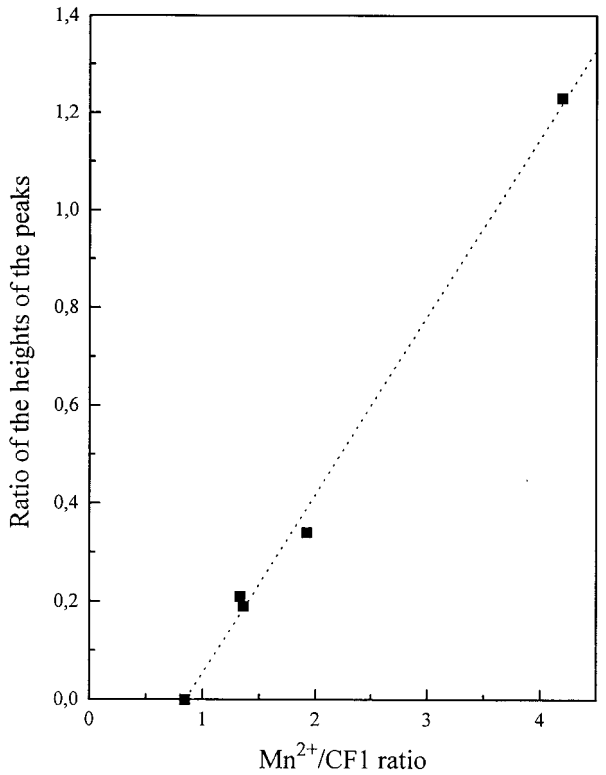

FIGURE 8: Ratio of the amplitude of the ~2 MHz peak with that of the 8.6 MHz peak in ESEEM spectra of samples containing Mn(II) and CF1 with different Mn/CF1 contents. The measurements were performed on spectra similar to that in Figure 6B. The dotted line is the linear regression of the data points.

It is shown above that TF1 supplemented with 3 Mn/TF1 shows Mn(II) coordinated with ^{14}N ligands possibly from a lysine residue. Addition of ATP to such a sample shows the appearance of a peak at 8.2 MHz (not shown), a situation that is similar to that shown in Figure 5B for the sample with only the M1 site filled with Mn(II). This was interpreted as indicating binding of a phosphate group from ATP to the Mn(II) ion. Because the ESEEM spectrum of the sample with 3 Mn/TF1 is the superposition of the ESEEM spectra of the three Mn(II) ions that bind to TF1 and because these might bind in a different manner, it was not possible to determine whether binding of phosphate from the added ATP occurred only for the M1 site or if the all three sites, M1−M3, involved binding by ATP.

DISCUSSION

The results reported above indicate that CF1 and TF1 can be prepared largely devoid of divalent metal cations by successive dialyses in the presence of EDTA. This treatment could be reversed by supplementing the metal-depleted proteins with Mg(II) or Mn(II), leading to enzymes with fully active ATPase activity. The relatively high concentration (10 mM) of EDTA used in this work is probably important to remove all the Mg(II) cations from the metal binding sites, since it is usually accepted that storage of CF1 as a precipitate in a 50% saturated solution of NH_4Cl with 2 mM EDTA leaves the M1 site with bound Mg(II) (Houseman et al., 1994a). The binding of Mn(II) ions to successive binding sites on CF1 and TF1 could be followed by EPR and ESEEM spectroscopy. For the CF1 complex and Mn/CF1 ratios of ~0.3−0.8, a first binding site is observed and characterized. The zero field splitting parameters, $|D| \approx 200 \times 10^{-4}$ cm^{-1} and $|E| \approx 40 \times 10^{-4}$ cm^{-1}, of Mn(II) bound to this site indicate a slight but significant deviation from octahedral symmetry. The $|D|$ parameter is in fact relatively small when compared with those for other protein Mn(II) sites published in the literature (Reed & Markham, 1984), indicating that the metal binding site that is filled first on CF1 is in a highly symmetric environment. This result is not surprising in view of the rather facile filling of the metal sites of CF1 by a range of different divalent metal cations with substantial retainment of ATPase/ATPsynthase activities (Hochman et al., 1976).

From measurements of the magnetic field dependence of the NMR spin−lattice relaxation rate of solvent protons in various Mn(II) complexes with CF1, Haddy et al. (1989) concluded that Mn(II) could bind to CF1 in two sites with approximately tetrahedral geometries. In their experiments, however, the CF1 complex was reported to retain Mg(II) cations in a ratio ~1 Mg/CF1. Thus the Mn(II) binding site that is studied in the present report is probably different from the Mn(II) sites described by Haddy et al. (1989) but is likely to correspond to the metal site with nonlabile endogenous Mg(II) in their enzyme, also known as the M1 site (Houseman et al., 1994a).

The ESEEM spectrum of Mn(II) in this M1 site is interpreted in terms of a phosphate ligand. In fact, phosphate groups that are present in purified CF1 belong to the strongly bound ADP molecule (Bruist & Hammes, 1981) that was not removed by the treatment with EDTA. The peak at ~8.6 MHz in the ESEEM of the Mn·CF1 complex measured at 3460 G is assigned to the $|M_S = -1/2; M_I = \pm 1/2>$ transition for the β-phosphate ^{31}P of this endogenous ADP with a hyperfine coupling $|A| \approx 5.3$ MHz. As noted above, other electronic transitions may also contribute to these frequencies, especially when measured at >3600 G. The ^{31}P assignment is based on the magnetic field dependence of the peak and also on the strong similarity of the spectrum with those reported for other protein complexes with nucleotides (LoBrutto et al., 1986, 1993; Eads et al., 1988; Tipton et al., 1989; Larsen et al., 1993). This indicates that the binding site N1 of the endogenous ADP in CF1 is very close to the Mn(II) binding site M1, with the β-phosphate coordinating the Mn(II) ion. The peak at 3.7 MHz in the ESEEM spectrum could also originate from coupling with the β-phosphate ^{31}P, with a specific assignment to the $|M_S = 1/2; M_I = \pm 1/2>$ hyperfine line of the $M_S = 1/2 \leftrightarrow M_S = 3/2$ transition. This is based on the theoretical treatment of the ESEEM spectra of Mn(II) complexes with *ras* p21 and GDP (Larsen et al., 1993). However, because the field dependence of the 3.7 MHz peak in the spectra of the Mn·CF1 complex is close to that expected for the Larmor frequency of ^{23}Na, we cannot exclude the possibility of dipolar coupling of the Mn(II) ion with a rather distant ^{23}Na atom in CF1.

There is no indication from the ESEEM spectra for a ^{14}N-containing ligand for Mn(II) bound to the M1 site in CF1, such as the bonding nitrogen of a histidine imidazole, as has been found for the Mn(II) sites in lectins (McCracken et al., 1991) and cytochrome *c* oxidase (Espe et al., 1995). Thus the other ligands of Mn(II) in the M1 metal binding site of CF1 are likely to be water molecules and/or carboxylates from, e.g., aspartates or glutamates. In this respect, the recently published crystal structure of MF1 at 2.8 Å resolution may provide a useful working scheme to interpret

the spectroscopic data reported here. In fact, the catalytic nucleotide binding site N1 with endogenous ADP in CF1 is likely to correspond to the β_{DP} site identified in the MF1 crystals. Thus the Mn(II) cation would be coordinated by amino acids near this nucleotide site, which are mainly from a β subunit (Abrahams et al., 1994). For MF1, the O_γ of β-Thr-163 and the β-phosphate from the ADP have been proposed as ligands to the Mg(II) cation, with water molecules as the probable remaining ligands (Abrahams et al., 1994). The spectroscopic results reported here are consistent with a model in which the ligand set of the Mn(II) site M1 with strongest affinity on CF1 is similar to that for the Mg(II) in the β_{DP} site on MF1.

The Mg(II) binding sites in TF1 are much less well studied than those in CF1; however, because the enzymatic properties of TF1 and CF1 are so similar, it is reasonable to postulate that metal binding sites exist in TF1 with properties similar with those in CF1. We have studied complexes of TF1 with Mn(II) in different stoichiometries in order to characterize these metal binding sites and to compare them with those in CF1. A complex of Mn(II) with TF1 (0.4 Mn/TF1) probably reflects the spectroscopic properties of a metal site that is analogous to the M1 site described above in CF1. In fact, such a complex showed an ESEEM spectrum that is interpreted in terms of a complex with nitrogen ligands (see below). This contrasts with the situation observed for CF1. However, after addition of ATP to such a sample, nuclear transitions from ^{31}P can be observed in the ESEEM spectrum that indicate binding of a phosphate from the added nucleotide to Mn(II) with $|A| \approx 4.5$ MHz. A hyperfine coupling of this magnitude is significantly smaller than that ($|A| \approx 5.3$ MHz) measured for the β-phosphorus of ADP bound to Mn(II) in CF1. Reasons for this difference may include conformational differences associated with binding of ADP or ATP and may reflect which phosphates coordinate Mn(II). For instance, a hyperfine coupling of ~4 MHz has been measured for the coupled ^{31}P in a Mn(II) complex of pyruvate kinase with ATP (Tipton et al., 1989), in which the coordinating phosphate is in γ position (Lodato & Reed, 1987). When the Mn·TF1·ATP complex was left to incubate for 15 min at room temperature before the ESEEM spectra were recorded, the measured hyperfine coupling with ^{31}P was larger ($|A| \approx 5.1$ MHz; Table 2). This is interpreted as reflecting a conformational change affecting the Mn(II) and nucleotide binding sites under conditions that favor unisite hydrolysis of ATP. As a conclusion, these results may also be interpreted using the framework of the structural data available for MF1: we propose that in TF1 the M1 site involves binding of Mn(II) by the O_γ of β-Thr-163 and the N_ϵ of deprotonated β-Lys-162. Our results suggest that after addition of ATP, a phosphate group from ATP coordinates the Mn(II), perhaps by replacing the amine ligand from the lysine, although the occurrence of a Mn·TF1·ATP complex with both ligands cannot be ruled out by our present data. Further, our results indicate that a change in the hyperfine coupling with the bound phosphate occurs after a 15 min incubation of the ternary complex at room temperature and that this probably reflects a change in the Mn(II) coordination. Certainly, more data from Mn(II) complexes with other phosphate-derived ligands are needed to further characterize this observation.

When Mn(II) is supplemented to the metal-depleted CF1 with Mn/CF1 ratios greater than 1, the ESEEM spectrum of the Mn·CF1 complex showed additional frequencies below ~5 MHz. This indicates that additional binding sites are filled in CF1, as unbound Mn(II) would exist mainly as the hexaaquomanganese(II) cation, with a spectrum that only displays the frequency of weakly coupled protons at $\nu_L \approx 14.73$ MHz for $H = 3460$ G. It was not possible however to quantify these additional Mn(II) binding sites, as the amplitudes of the peaks in the FT ESEEM are not expected to scale with the amount of bound Mn(II) in the sample. However, it is likely that at least some of the additional Mn(II) binding sites that are observed here correspond to the additional metal binding sites with strong affinity and described as M2 and M3 by Houseman et al. (1994a). Because these sites are expected to fill after M1 is filled with Mn(II) (see above), the ESEEM spectra of CF1 samples with, e.g., 3 Mn/CF1 will provide information on the average coordination of the three filled Mn sites. Quantitative interpretation of the ESEEM spectra is not yet possible due to the complexity of the magnetic interaction of nuclear spins with an $S = {}^5/_2$ paramagnet, in particular of ^{14}N with $I = 1$. However, the additional frequencies below ~5 MHz in the ESEEM spectra of CF1 are attributed to the interaction with a nitrogen ligand, based on the magnetic field dependence of the ESEEM frequencies, and the similarity of the spectra with Mn(II) complexes with nitrogen donors, such as imidazole, poly-L-lysine, or glycine. Because this similarity is more pronounced with the glycine or the poly-L-lysine Mn(II) complexes, it is suggested that the M2 and M3 metal sites involve a protein residue with a nitrogen donor from a primary amine. This could originate from a deprotonated lysine ligand. Imidazole from histidines can also probably be ruled out as ligands to the M2 and M3 sites because of the absence of the strong transition at ~5 MHz that is observed for the interaction of Mn(II) with an imidazole nitrogen (see Figure 4). On the basis of EPR and ESEEM results obtained for CF1 complexes with VO(II), it has been suggested that a lysine residue provides a ligand to the VO(II) in the M2 and/or M3 sites, which could correspond to α-Lys-175 and β-Lys-162, respectively (Houseman et al., 1994a, 1995). The results reported here with Mn(II) in the M2 and M3 sites substantiate this earlier suggestion. The absence of frequencies other than those originating from ^{14}N in the ESEEM spectra also suggests that the other ligands to the Mn(II) in the M2 and M3 sites are probably oxygen donors.

Structural data on the metal binding sites of CF1 have been reported from EXAFS studies of complexes of Mn(II) with CF1 and ATP (Carmeli et al., 1986). The data on the complex with Mn(II) bound to the three tight binding sites (probably M1−M3) were analyzed in terms of an average Mn···O distance of 2.05 ± 0.15 Å, a distance that is significantly smaller than the average distance 2.15 ± 0.15 Å found for hexaaquomanganese(II). The results reported here from Q-band EPR spectroscopy on a slightly distorted Mn(II) site on CF1 are consistent with these earlier data. In addition, the authors found a Mn···P distance of 4.95 ± 0.15 Å which was attributed to the formation of the ternary complex Mn·CF1·ATP upon addition of ATP. The ESEEM results reported in this work on TF1 show that indeed such a ternary complex does form in the strong-affinity metal binding site M1 and that the formation of this complex may be of catalytic significance.

ACKNOWLEDGMENT

We thank Prof. Georges Calas for the use of his Q-band EPR spectrometer and Dr. Guillaume Morin for recording the EPR data at Q-band. We thank Ms. Véronique Mary and Jeannine Le Cruër for the preparation of CF1, Ms. Sandra Andrianambinintsoa, Nadège Koubbi, and Anne-Laure Chaissé for the preparation of TF1, Dr. Gérard Berger for extremely useful discussions and for communicating results prior to publication, and Dr. Paul Mathis for his interest and continuous support of this work.

REFERENCES

Abrahams, J. P., Leslie, A. G. W., Lutter, R., & Walker, J. E. (1994) *Nature 370*, 621−628.
Berger, G., Girault, G., André, F., & Galmiche, J. M. (1987) *J. Liquid Chromatogr. 10*, 1507−1517.
Berger, G., Girault, G., & Galmiche, J. M. (1990) *J. Liquid Chromatogr. 13*, 4067−4080.
Berger, G., Girault, G., Galmiche, J. M., & Pezennec, S. (1994*) J. Bioenerg. Biomembr.* 26, 335−346.
Bianchet, M., Ysern, X., Hullihen, J., Pedersen, P. L., & Amzel, M. L. (1991) *J. Biol. Chem. 266*, 21197−21201.
Boyer, P. D. (1993) *Biochim. Biophys. Acta 1140*, 215−250.
Bradford, M. (1976) *Anal. Biochem. 72*, 248−254.
Bruist, M. F., & Hammes, G. G. (1981) *Biochemistry 20*, 6298−6305.
Carmeli, C., Huang, J. Y., Mills, D. M., Jagendorf, A. T., & Lewis, A. (1986) *J. Biol. Chem. 261*, 16969−16975.
Cross, R. L. (1988) *J. Bioenerg. Biomembr. 20*, 395−406.
Cross, R. L. (1992) in *Molecular Mechanisms in Bioenergetics* (Ernster, L., Ed.), pp 317−330, Elsevier, Amsterdam.
Cross, R. L., & Nalin, C. M. (1982) *J. Biol. Chem. 257*, 2874−2881.
Eads, C. D., LoBrutto, R., Kumar, A., & Villafranca, J. J. (1988) *Biochemistry 27*, 165−170.
Espe, M. P., Hosler, J. P., Ferguson-Miller, S., Babcock, G. T., & McCracken, J. (1995) *Biochemistry 34*, 7593−7602.
Frasch, W. D., & Selman, B. R. (1982) *Biochemistry 21*, 3636−3643.
Fauth, J. M., Schweiger, A., Braunschweiler, L., Forrer, J., & Ernst, R. R. (1986) *J. Magn. Reson. 66*, 74−85.
Futai, M., Noumi, T., & Maeda, M. (1989) *Annu. Rev. Biochem. 58*, 111−136.
Girault, G., Berger, G., Galmiche, J. M., & André, F. (1988) *J. Biol. Chem. 263*, 14690−14695.
Haddy, A. E., & Sharp, R. R. (1989) *Biochemistry 28*, 3656−3664.
Haddy, A. E., Frasch, W. D., & Sharp, R. R. (1985) *Biochemistry 24*, 7926−7930.
Haddy, A. E., Frasch, W. D., & Sharp, R. R. (1989) *Biochemistry 28*, 3664−3669.
Halkides, C. J., Farrar, C. T., Larsen, R. G., Redfield, A. G., & Singel, D. J. (1994) *Biochemistry 33*, 4019−4035.
Hiller, R., & Carmeli, C. (1985) *J. Biol. Chem. 260*, 1614−1617.
Hochman, Y., & Carmeli, C. (1981) *Biochemistry 20*, 6287−6292.
Hochman, Y., Lanir, A., & Carmeli, C. (1976) *FEBS Lett. 61*, 255−259.
Houseman, A. L. P., Morgan, L., LoBrutto, R., & Frasch, W. D. (1994a) *Biochemistry 33*, 4910−4917.
Houseman, A. L. P., LoBrutto, R., & Frasch, W. D. (1994b) *Biochemistry 33*, 10000−10006.
Houseman, A. L. P., LoBrutto, R., & Frasch, W. D. (1995) *Biochemistry 34*, 3277−3285.
Kagawa, Y., & Yoshida, M. (1979) *Methods Enzymol. 55*, 781−787.
Kevan, L. (1990) in *Modern Pulsed and Continuous-Wave Electron Spin Resonance* (Kevan, L., & Bowman, M. K., Eds.) pp 231−266, Wiley Interscience, New York.
Larsen, R. G., Halkides, C. J., & Singel, D. J. (1993) *J. Chem. Phys. 98*, 6704−6721.
Latwesen, D. G., Poe, M., Leigh, J. S., & Reed, G. H. (1992) *Biochemistry 31*, 4946−4950.
LoBrutto, R., Smithers, G. W., Reed, G. H., Orme-Johnson, W. H., Tan, S. L., & Leigh, J. S. (1986) *Biochemistry 25*, 5654−5660.
LoBrutto, R., Digel, J., Latwesen, D. G., & Reed, G. H. (1993) *Proceedings of the International EPR Symposium, 35th Rocky Mountain Conference on Analytical Chemistry*, Denver, CO, July 1993.
Lodato, D. T., & Reed, G. H. (1987) *Biochemistry 26*, 2243−2250.
Markham, G. D., Nageswara Rao, B. D., & Reed, G. H. (1979) *J. Magn. Reson. 33*, 595−602.
McCracken, J., Peisach, J., Bhattacharyya, L., & Brewer, F. (1991) *Biochemistry 30*, 4486−4491.
Mims, W. B. (1984) *J. Magn. Reson. 59*, 291−306.
Mims, W. B., & Peisach, J. (1981) in *Biological Magnetic Resonance* (Berliner, L. J., & Reuben, J., Eds.) Vol. 3, pp 213−263, Plenum Press, New York.
Moroney, J. V., Lopresti, L., McEwen, B. F., McCarty, R. E., & Hammes, G. G. (1983) *FEBS Lett. 158*, 58−62.
Ohta, S., Tsuboi, M., Oshima, T., Yoshida, M., & Kagawa, Y. (1980) *J. Biochem. 87*, 1609−1617.
Ohta, S., Yohda, M., Ishizuka, M., Hirata, H., Hamamoto, T., Otawara-Hamamoto, Y., Matsuda, K., & Kagawa, Y. (1988) *Biochim. Biophys. Acta 933*, 141−155.
Pezennec, S., Berger, G., Andrianambinintsoa, S., Radziszewski, N., Girault, G., Galmiche, J. M., & Bäuerlein, E. (1995) *Biochim. Biophys. Acta 1231*, 98−110.
Reed, G. H., & Leyh, T. S. (1980) *Biochemistry 19*, 5472−5480.
Reed, G. H., and Markham, G. D. (1984) in *Biological Magnetic Resonance* (Berliner, L. J., & Reuben, J., Eds.) Vol. 6, pp 73−142, Plenum Press, New York.
Richter, M. L., Patrie, W. J., & McCarty, R. E. (1984) *J. Biol. Chem. 259*, 7371−7373.
Senior, A. E. (1990) *Annu. Rev. Biophys. Biophys. Chem. 19*, 7−41.
Shapiro, A. B., Huber, A. H., & McCarty, R. E. (1991) *J. Biol. Chem. 266*, 4194−4200.
Tipton, P. A., & Peisach, J. (1991) *Biochemistry 30*, 739−744.
Tipton, P. A., McCracken, J., Cornelius, J. B., & Peisach, J. (1989) *Biochemistry 28*, 5720−5728.
Wise, J. G., Duncan, T. M., Latchney, L. R., Cox, D. N., & Senior, A. E. (1983) *Biochem. J. 215*, 343−350.
Xue, Z., Zhou, J. M., Melese, T., Cross, R. L., & Boyer, P. D. (1987) *Biochemistry 32*, 9866−9873.

BI960532L